

# Razvejitve pri Van der Pol-Duffingovem nihalu

## Bifurcations of the Van der Pol-Duffing Oscillator

Rudolf Pušenjak

*Metoda koračnega harmonskega ravnovesja se je izkazala za učinkovito orodje pri računanju periodičnih nihanj v analizi nelinearnih dinamičnih sistemov. Razvili smo jo v obliko, ki omogoča izračun ustaljenega periodičnega odziva v odvisnosti od različnih spremenljivih parametrov. Kadar razvejitveni postopek sledi zaporedju podvojitvev period, je periodični odziv sestavljen iz subharmoničnih rešitev višjih stopenj. Ko v postopku podvojitvev period ne obstajajo več nobene subharmonične rešitve, se periodični odziv spremeni v kaotičnega. Spreminjanje amplitud periodičnega nihanja v odvisnosti od spremenljivih parametrov sistema in s tem možen prehod v kaos prikazujemo v razvejitvenih diagramih. Splošni postopek konstrukcije razvejitvenega diagrama je uporabljen pri van der Pol-Duffingovem nihalu za različne vrste parametrov. Izkaže se, da se pri van der Pol-Duffingovem nihalu pojavi vrsta različnih razvejitvev, ki jih je mogoče analizirati le z uporabo ustreznih strategij.*

© 2003 Strojniški vestnik. Vse pravice pridržane.

**(Ključne besede: metode koračnega harmonskega ravnovesja, sistemi dinamični, sistemi nelinearni, diagrami razvejitveni)**

*The incremental harmonic balance method has proved to be an efficient tool for computing periodic oscillations in the analysis of nonlinear dynamical systems. It was developed into a form that enables the computing of steady-state periodic response with a dependence on various variable parameters. When the bifurcation process follows a sequence of period doublings, then the periodic response is composed of subharmonic solutions of higher orders. When no more subharmonic solutions exist in the process of periodic doublings, then the periodic response becomes chaotic. The changing of the amplitudes of the periodic oscillation in dependence of the variable system parameters and the possible transition into chaos is shown in bifurcation diagrams. A general procedure for the construction of a bifurcation diagram is the used in van der Pol-Duffing oscillator for various kinds of parameters. It is proved that the van der Pol-Duffing oscillator possesses various kinds of bifurcations, which can be analyzed by using suitable strategies.*

© 2003 Journal of Mechanical Engineering. All rights reserved.

**(Keywords: incremental harmonic balance method, dynamical systems, nonlinear systems, bifurcation diagrams)**

### 0 UVOD

Metoda koračnega harmonskega ravnovesja (MKHR) je postopek za izračun ustaljenega periodičnega odziva nelinearnega dinamičnega sistema [1], ki ne uporablja časovne, temveč frekvenčno domeno. Časovni potek periodičnega odziva je diskretiziran s pripadajočimi komponentami Fourierjevega spektra. Diskretiziran potek uporabimo v koračni enačbi, ki jo izpeljemo iz vodilne enačbe z uporabo razvoja v Taylorjevo vrsto. Uporaba Galerkinovega postopka na koračni enačbi privede na sistem linearnih algebrskih enačb za neznane prirastke Fourierjevih koeficientov. Sistem algebrskih enačb vsebuje poleg neznanih prirastkov Fourierjevih koeficientov še prirastke različnih sistemskih parametrov. Celotni sistem enačb rešujemo iterativno po Newton-Raphsonovi

### 0 INTRODUCTION

The incremental harmonic balance method (IHBM) is a procedure for computing the steady-state periodic response of a nonlinear dynamical system [1] in which the frequency domain applies instead of the time domain. The time response of the periodic response is discretized by the corresponding components of the Fourier spectrum. The discretized form is used in an incremental equation, which is derived from the governing equation by a Taylor series expansion. The application of the Galerkin procedure on the incremental equation leads to the system of a linear algebraic equation for unknown increments of the Fourier coefficients. This system contains, in addition to unknown increments of the Fourier coefficients, increments of various system parameters. The complete system of equations is solved iteratively

metodi. Postopek povečave [1] dovoljuje, da ne izračunamo le posamezne rešitve, temveč lahko spremljamo potek rešitev v odvisnosti od spremenljivega parametra. Dve vrsti prirastkov sistemskih parametrov zavzemata posebno mesto: prva vrsta so prirastki vzbujevalne frekvence, drugi pa prirastki amplitud vzbujevalne sile. Razvejitvene diagrame konstruiramo navadno tako, da spreminjamo le en parameter naenkrat. Glede na omenjeni vrsti prirastkov izhajata od tod dve vrsti razvejitvenih diagramov, ki sta obenem najpogostejši. Prva vrsta razvejitvenih diagramov so resonančne krivulje, druga pa odzivne krivulje v odvisnosti od spremenljive amplitude vzbujevalne sile.

V resonančnih krivuljah nekaterih nelinearnih dinamičnih sistemov, kakor so nihala Duffingovega tipa, deluje nelinearnost tako, da se vsiljena frekvenca pri največji amplitudi tem bolj razlikuje od frekvence lastnega nihanja, čim večja je stopnja nelinearnosti. To ima za posledico, da se vrh resonančne krivulje upogne na eno ali drugo stran glede na lego, ki jo vrh resonančne krivulje zavzema v linearnem sistemu. Upogibanje resonančnih krivulj povzroča obračanje poteka krivulje, nastajanje histerez in zank ter funkcijsko večličnost v določenem območju parametrov. Omenjene točke imenujemo obračališča ali točke zrcaljenja. V moderni razvejitveni teoriji [2] jih prištevamo k razvejitvenim točkam, čeprav v njih ne nastajajo nove veje kakovostno različnih rešitev. Značilnost obračališč je, da v njih veje stabilnih rešitev izgubijo stabilnost ali nasprotno.

V razvejitvenem diagramu, ki prikazuje odvisnost izbrane skalarne veličine, na primer vrednosti amplitude ob koncu vsake periode periodičnega nihanja od vzbujevalne sile, se lahko poleg obračališč pojavijo še druge razvejitvene točke. Le-te so izraz različnih mehanizmov, ki vplivajo na potek nihanja. Na primer, če se v frekvenčnem spektru periodičnega nihanja nelinearnega nihala pojavljajo le lihe harmonske komponente, je odziv simetričen. Nelinearno nihalo lahko v določeni točki izgubi lastnost simetrije, zaradi česar se v frekvenčnem spektru poleg lihkih pojavijo še sode harmonske komponente, točko, v kateri se pojavi omenjeni pojav, pa imenujemo razvejitveno točko izgube simetrije. Točke, v katerih se v frekvenčnem spektru pojavijo subharmonske, ki ustrezajo dvojnemu trajanju periode nelinearnega nihanja, imenujemo točke podvojitvev period. Točke, v katerih ravnotežne točke preidejo v mejne zanke periodičnega nihanja, imenujemo Hopfove razvejitvene točke.

Določitev obračališč, razvejitvenih točk izgube simetrije, točk podvojitvev period in Hopfovih razvejitvenih točk je ozko povezana s stabilnostjo periodičnih rešitev. Stabilnost periodičnih rešitev presojamo s Floquetovo teorijo [3].

by the Newton–Raphson method. The augmentation procedure [1] allows us not only to calculate a particular solution, but the evolution of the solutions can be followed with the dependence on the variable parameter. Two kinds of system-parameter increments play a significant role: the first are the excitation frequency increments, and the second are the increments of the excitation force amplitudes. Bifurcation diagrams are usually constructed by changing one parameter at a time. For both kinds of increments two types of bifurcation diagram result, the division being roughly equal. The first kind of bifurcation diagrams are resonance curves, and the second are response curves, with a dependence on the variable amplitude of the excitation force.

In the resonance curves of some nonlinear dynamic systems, such as oscillators of the Duffing type, the nonlinearity acts so that the forced frequency at maximum amplitude differs more from the free oscillation frequency as the degree of nonlinearity increases. Consequently, the resonance peak bends on one or other side of the site, where the resonance peak takes place in the linear system. The bending of the resonance peaks causes turning of the resonance courses, an increase in the hysteresis and loops as well as the multi-valuedness of the response in the specified region of the parameters. The aforementioned points are called turning points or folds. In contemporary bifurcation theory [2] the folds are added up to the bifurcation points, although new branches of the qualitatively different solutions do not arise. The characteristic for turning points is that the branches of stable solutions lose their stability at these points, and vice versa.

In a bifurcation diagram, which represents the dependence of the selected scalar quantity, for example, the value of the amplitude at the end of each period on the excitation force, other bifurcation points, such as turning points, can appear. These bifurcation points are a consequence of various mechanisms, which have an influence on the course of the oscillation. For example, when a nonlinear oscillator performs a periodic oscillation with a frequency spectrum containing only odd harmonic components the response is symmetrical. A nonlinear oscillator can lose symmetry properties in the fixed point, which causes the appearance of even harmonic components in the frequency spectrum. The point where this happens is called the symmetry breaking point. Points where the subharmonics appear in the frequency spectrum, which correspond to the doubled duration of the period, are called period doubling points. Points where the equilibrium points go over to the limit cycle of the periodic oscillation are called Hopf bifurcation points.

The determination of turning points, symmetry breaking points, period doubling points and Hopf bifurcation points is closely connected with the stability of periodic solutions. The stability of periodic solutions is examined with the aid of the Floquet theory [3].

Van der Pol–Duffingovo nihalo je nelinearni dinamični sistem z eno prostostno stopnjo, katerega periodična nihanja so mnogo proučevali tako iz analitičnega kakor eksperimentalnega vidika. V pričujočem prispevku bomo obravnavali periodična nihanja van der Pol–Duffingovega nihala z uporabo MKHR s poudarkom na konstrukciji razvejitvenih diagramov. Pokazali bomo, da se pojavijo pri tem nihalu vse zgoraj omenjene razvejitve. Videli bomo tudi, da je poleg MKHR treba razviti vrsto strategij, ki omogočajo analizo posameznih vrst razvejitvenih točk.

### 1 PRILAGODITEV MKHR ZA SLEDENJE POTEKA PO VEJAH RAZVEJITVENEGA DIAGRAMA

MKHR je bila za nelinearne dinamične sisteme z več prostostnimi stopnjami razvita v [1]. Zaradi udobnosti bomo tukaj predstavili najpomembnejše značilnosti metode. Nelinearne dinamične sisteme z  $N$  prostostnimi stopnjami, ki jih periodično vzbujamo s kombinacijo  $M_i$  komenzurnih harmoničnih signalov, opišemo z diferencialno enačbo

$$\frac{d^2\mathbf{q}}{dt^2} + \mathbf{h}\left(\mathbf{q}(t), \frac{d\mathbf{q}}{dt}, \omega, \lambda\right) = \sum_{n=1}^{M_i} \left(\mathbf{f}_n^c \cos n\omega t - \mathbf{f}_n^s \sin n\omega t\right) \quad (1),$$

kjer je  $\mathbf{q} = \{q_1, \dots, q_N\}^T$  vektor generaliziranih koordinat,  $\mathbf{h} = \{h_1, \dots, h_N\}^T$  vektor nelinearnih funkcij, ki ustreza delovanju sil v nelinearnih elementih sistema,  $\lambda = \{\lambda_1, \dots, \lambda_p\}^T$  je vektor prostih parametrov sistema,  $\mathbf{f}_n^c = \{f_{n1}^c, \dots, f_{nN}^c\}^T$ ,  $\mathbf{f}_n^s = \{f_{n1}^s, \dots, f_{nN}^s\}^T$  sta amplitudna vektorja, ki pripadata  $n$ -ti harmonski komponenti vzbujevalne sile,  $\omega$  je vzbujevalna frekvenca in  $t$  čas. Z uvedbo brezrazsežnega časa  $\tau = \omega t$  enačbo (1) prevedemo v obliko:

$$\omega^2 \frac{d^2\mathbf{q}}{d\tau^2} + \mathbf{h}\left(\mathbf{q}(\tau), \omega \frac{d\mathbf{q}}{d\tau}, \omega, \lambda\right) = \sum_{n=1}^{M_i} \left(\mathbf{f}_n^c \cos n\tau - \mathbf{f}_n^s \sin n\tau\right) \quad (2)$$

ter jo z razvojem vseh členov enačbe v Taylorjevo vrsto lineariziramo tako, da obdržimo izraze, ki so linearni v posameznih prirastkih:

$$\begin{aligned} & (\omega + \Delta\omega)^2 \frac{d^2(\mathbf{q} + \Delta\mathbf{q})}{d\tau^2} + \mathbf{h}\left[\mathbf{q} + \Delta\mathbf{q}, (\omega + \Delta\omega) \frac{d(\mathbf{q} + \Delta\mathbf{q})}{d\tau}, \omega + \Delta\omega, \lambda + \Delta\lambda\right] \\ &= (\omega^2 + 2\omega\Delta\omega + \dots) \frac{d^2\mathbf{q}}{d\tau^2} + \omega^2 \frac{d^2\Delta\mathbf{q}}{d\tau^2} + \mathbf{h}\left[\mathbf{q}, \omega \frac{d\mathbf{q}}{d\tau}, \omega, \lambda\right] + \frac{\partial\mathbf{h}}{\partial\mathbf{q}} \Delta\mathbf{q} + \omega \frac{\partial\mathbf{h}}{\partial\left(\frac{d\mathbf{q}}{d\tau}\right)} \frac{d\Delta\mathbf{q}}{d\tau} + \frac{\partial\mathbf{h}}{\partial\omega} \Delta\omega + \frac{\partial\mathbf{h}}{\partial\lambda} \Delta\lambda \\ &= \omega^2 \frac{d^2\mathbf{q}}{d\tau^2} + 2\omega\Delta\omega \frac{d^2\mathbf{q}}{d\tau^2} + \omega^2 \frac{d^2\Delta\mathbf{q}}{d\tau^2} + \mathbf{h}\left[\mathbf{q}, \omega \frac{d\mathbf{q}}{d\tau}, \omega, \lambda\right] + \omega\mathbf{G}_{N1} \frac{d\Delta\mathbf{q}}{d\tau} + \mathbf{G}_{N2}\Delta\mathbf{q} + \frac{\partial\mathbf{h}}{\partial\omega} \Delta\omega + \mathbf{G}_{N3}\Delta\lambda \\ &= \sum_{n=1}^{M_i} \left[ (\mathbf{f}_n^c + \Delta\mathbf{f}_n^c) \cos n\tau - (\mathbf{f}_n^s + \Delta\mathbf{f}_n^s) \sin n\tau \right] \end{aligned} \quad (3),$$

pri čemer upoštevamo, da odvajanje  $N$ -komponentnega vektorja  $\mathbf{h}$  po  $N$ -komponentnih

A van der Pol–Duffing oscillator is a nonlinear dynamical system with one degree of freedom, the periodic oscillations of which are much studied from both the analytical as well as from the experimental point of view. In this paper the periodic oscillations of a van der Pol–Duffing oscillator will be treated by using IHBM, with an emphasis on the construction of the bifurcation diagrams. We will show that a lot of the aforementioned bifurcations take place in this type of oscillator. It is also shown that besides IHBM one needs a lot of strategies that can be used to analyze particular kinds of bifurcation points.

### 1 THE ADAPATION OF IHBM FOR BRANCH TRACING THROUGH A BIFURCATION DIAGRAM

IHBM has been developed for nonlinear dynamical systems with many degrees of freedom [1]. For convenience, the most important characteristics of the method will be repeated here. Nonlinear dynamical systems with  $N$  degrees of freedom, which are periodically excited by the combination of  $M_i$  commensurate harmonic signals, are described by the differential equation

where  $\mathbf{q} = \{q_1, \dots, q_N\}^T$  is the vector of generalized coordinates,  $\mathbf{h} = \{h_1, \dots, h_N\}^T$  is the vector of continuous and derivable nonlinear functions corresponding to the acting of generalized forces in elements of the nonlinear system,  $\lambda = \{\lambda_1, \dots, \lambda_p\}^T$  is the vector of free system parameters,  $\mathbf{f}_n^c = \{f_{n1}^c, \dots, f_{nN}^c\}^T$ ,  $\mathbf{f}_n^s = \{f_{n1}^s, \dots, f_{nN}^s\}^T$  are the amplitude vectors, which correspond to the  $n^{\text{th}}$  harmonic of the exciting force,  $\omega$  is the exciting frequency and  $t$  is the time. Introducing the nondimensional time  $\tau = \omega t$ , Equation (1) can be rewritten in the form:

and linearized by expanding its terms in Taylor series so that only expressions that are linear in several increments are retained:

where the derivatives of  $N$ , vector  $\mathbf{h}$ , upon  $N$ , vectors  $\dot{\mathbf{q}} = d\mathbf{q}/d\tau$  and  $\mathbf{q}$ , respectively, define two  $N \times N$

vektorjih  $\dot{\mathbf{q}} = d\mathbf{q}/d\tau$  oziroma  $\mathbf{q}$  definira dve  $N \times N$  matriki  $\mathbf{G}_{N1}$  in  $\mathbf{G}_{N2}$ . Indeks  $N$  v obeh matrikah pomeni, da sta matriki v  $\dot{\mathbf{q}}$  oziroma  $\mathbf{q}$  nelinearni. Podobno dobimo z odvajanjem vektorja  $\mathbf{h}$  po vektorju  $\lambda$  matriko  $\mathbf{G}_{N3}$ . Po ureditvi dobimo koračno enačbo:

$$\omega^2 \frac{d^2 \Delta \mathbf{q}}{d\tau^2} + \omega \mathbf{G}_{N1} \frac{d \Delta \mathbf{q}}{d\tau} + \mathbf{G}_{N2} \Delta \mathbf{q} = \sum_{n=1}^{M_l} \left[ \left( \mathbf{f}_n^c + \Delta \mathbf{f}_n^c \right) \cos n\tau - \left( \mathbf{f}_n^s + \Delta \mathbf{f}_n^s \right) \sin n\tau \right] - \omega^2 \frac{d^2 \mathbf{q}}{d\tau^2} - \mathbf{h} \left[ \mathbf{q}, \omega \frac{d\mathbf{q}}{d\tau}, \omega, \lambda \right] - \left( 2\omega \frac{d^2 \mathbf{q}}{d\tau^2} + \frac{\partial \mathbf{h}}{\partial \omega} \right) \Delta \omega - \mathbf{G}_{N3} \Delta \lambda \quad (4)$$

Ustaljeno periodično nihanje zapišemo v obliki Fourierjeve vrste, v kateri zadržimo iz praktičnih razlogov le končno število členov. Vrsto zapišemo v zgoščeni matrični obliki:

$$\mathbf{q}(\tau) = \text{diag}(\mathbf{T}) \cdot \mathbf{a} = \mathbf{Y} \cdot \mathbf{a} \quad (5)$$

kjer je  $\mathbf{Y} N \times N N_h$  matrika, sestavljena tako, da se vzdolž diagonale  $N$ -krat ponovi matrika  $\mathbf{T}$ . Pri tem velja:

$$\mathbf{T} = [\mathbf{T}^c, \mathbf{T}^s], \mathbf{a} = \left\{ \mathbf{a}^{1T}, \mathbf{a}^{2T}, \dots, \mathbf{a}^{N^T} \right\}^T, \mathbf{a}^{iT} = \left\{ a_{0^i}, a_{1^i}, \dots, a_{N^c}^i, b_{0^i}, \dots, b_{N^s}^i \right\}^T, (i=1, \dots, N) \quad (6)$$

in

$$\mathbf{T}^c = \left[ 1, \cos \frac{\tau}{m}, \dots, \cos \frac{N^c \tau}{m} \right], \mathbf{T}^s = \left[ 0, \sin \frac{\tau}{m}, \dots, \sin \frac{N^s \tau}{m} \right] \quad (7)$$

V enačbi (7) sta  $N^c, N^s$  števili, ki označujeta najvišjo stopnjo kosinusnih oziroma sinusnih členov, ki jih obdržimo v okrnjeni Fourierjevi vrsti, medtem ko  $N_h$  pomeni število vseh harmonskih členov matrike  $\mathbf{T}$ . Število  $m$  je subharmonski indeks, s katerim lahko izrazimo subharmonične rešitve. Z uvrstitvijo enačbe (5) v enačbo (4) dobimo:

$$\left( \omega^2 \frac{d^2 \mathbf{Y}}{d\tau^2} + \omega \mathbf{G}_{N1} \frac{d \mathbf{Y}}{d\tau} + \mathbf{G}_{N2} \mathbf{Y} \right) \cdot \Delta \mathbf{a} = \sum_{n=1}^{M_l} \left[ \left( \mathbf{f}_n^c + \Delta \mathbf{f}_n^c \right) \cos n\tau - \left( \mathbf{f}_n^s + \Delta \mathbf{f}_n^s \right) \sin n\tau \right] - \left( \omega^2 \frac{d^2 \mathbf{Y}}{d\tau^2} \cdot \mathbf{a} + \mathbf{h} \left[ \mathbf{Y} \cdot \mathbf{a}, \omega \frac{d \mathbf{Y}}{d\tau} \cdot \mathbf{a}, \omega, \lambda \right] \right) - \left( 2\omega \frac{d^2 \mathbf{Y}}{d\tau^2} \cdot \mathbf{a} + \frac{\partial \mathbf{h}}{\partial \omega} \right) \Delta \omega - \mathbf{G}_{N3} \Delta \lambda \quad (8)$$

Na dobljeni enačbi izvedemo Galerkinov postopek tako, da enačbo premultipliramo s poljubno variacijo  $\delta \mathbf{a}^T \mathbf{Y}^T$ , nato pa integriramo v mejah od 0 do  $2m\pi$ . S tem dobimo linearno algebrsko enačbo v neznanih prirastkih Fourierjevih koeficientov:

$$\mathbf{H} \cdot \Delta \mathbf{a} = \mathbf{R} + \Delta \mathbf{F} - \mathbf{Q}(\omega) \Delta \omega - \mathbf{P}(\lambda) \Delta \lambda \quad (9)$$

kjer je  $\mathbf{H} N N_h \times N N_h$  tangentialna matrika:

$$\mathbf{H} = \frac{1}{m\pi} \int_0^{2m\pi} \left( \omega^2 \mathbf{Y}^T \frac{d^2 \mathbf{Y}}{d\tau^2} + \omega \mathbf{Y}^T \mathbf{G}_{N1} \frac{d \mathbf{Y}}{d\tau} + \mathbf{Y}^T \mathbf{G}_{N2} \mathbf{Y} \right) d\tau = -\omega^2 \mathbf{M} + \omega \mathbf{C} + \mathbf{K} \quad (10)$$

ki je sestavljena iz deležev matrike  $\mathbf{M}$ :

$$\mathbf{M} = -\frac{1}{m\pi} \int_0^{2m\pi} \mathbf{Y}^T \frac{d^2 \mathbf{Y}}{d\tau^2} d\tau \quad (11)$$

nelinearne matrike  $\mathbf{C}$ , ki pripada členom dušenja v enačbi (1):

matriki  $\mathbf{G}_{N1}$  and  $\mathbf{G}_{N2}$ . The index  $N$  means that both matrices are nonlinear in  $\dot{\mathbf{q}}$  and  $\mathbf{q}$ , respectively. Analogously, the derivative of vector  $\mathbf{h}$  upon vector  $\lambda$  gives a matrix  $\mathbf{G}_{N3}$ . After rearrangement one obtains the incremental equation:

The steady-state periodic oscillation is represented in the form of a Fourier series, where for practical reasons only a finite number of terms is used. The series is written in a compact matrix form:

where  $\mathbf{Y}$  is a  $N \times N N_h$  matrix, which is composed by repeating the matrix  $\mathbf{T}$  along the main diagonal. For this it holds that:

and

The numbers  $N^c, N^s$  in Equation (7) denote highest order of cosine and sine terms, retained in a truncated Fourier series, and  $N_h$  denotes the number of all the harmonic terms in matrix  $\mathbf{T}$ . The number  $m$  is a subharmonic index, which is used to express subharmonic solutions. Putting Equation (5) into equation (4) one obtains:

For this equation the Galerkin procedure is applied so that the equation is premultiplied by an arbitrary variation  $\delta \mathbf{a}^T \mathbf{Y}^T$  and then integrated over the interval from 0 to  $2m\pi$ . The result of the Galerkin procedure is a linear algebraic equation in unknown Fourier coefficient increments:

where  $\mathbf{H}$  is a  $N N_h \times N N_h$  tangential matrix:

which is composed from parts of the matrix  $\mathbf{M}$ :

from the nonlinear matrix  $\mathbf{C}$ , which corresponds to the damping terms in Equation (1):

$$\mathbf{C} = \frac{1}{m\pi} \int_0^{2m\pi} \left( \mathbf{Y}^T \mathbf{G}_{N1} \frac{d\mathbf{Y}}{d\tau} \right) d\tau \quad (12)$$

in nelinearne matrice  $\mathbf{K}$ , ki pripada togostnim členom and from the nonlinear matrix  $\mathbf{K}$ , which corresponds to the stiffness terms in Equation (1):

$$\mathbf{K} = \frac{1}{m\pi} \int_0^{2m\pi} \mathbf{Y}^T \mathbf{G}_{N2} \mathbf{Y} d\tau \quad (13)$$

Desno stran enačbe (9) sestavljajo vektor ostankov: The right side of Equation (9) is combined from the residual vector:

$$\mathbf{R} = \frac{1}{m\pi} \int_0^{2m\pi} \left[ \sum_{n=1}^{M_i} \mathbf{Y}^T \left( \mathbf{f}_n^c \cos n\tau - \mathbf{f}_n^s \sin n\tau \right) \right] d\tau - \frac{1}{m\pi} \left( \int_0^{2m\pi} \omega^2 \mathbf{Y}^T \frac{d^2 \mathbf{Y}}{d\tau^2} \cdot \mathbf{a} + \mathbf{Y}^T \cdot \mathbf{h} \left[ \mathbf{Y} \cdot \mathbf{a}, \omega \frac{d\mathbf{Y}}{d\tau} \cdot \mathbf{a}, \omega, \lambda \right] \right) d\tau \quad (14)$$

vektor prirastkov  $\Delta \mathbf{F}$ , ki ustreza komponentam from the increment vector  $\Delta \mathbf{F}$ , which corresponds to the incremental components of external forcing:

$$\Delta \mathbf{F} = \frac{1}{m\pi} \int_0^{2m\pi} \left[ \sum_{n=1}^{M_i} \mathbf{Y}^T \left( \Delta \mathbf{f}_n^c \cos n\tau - \Delta \mathbf{f}_n^s \sin n\tau \right) \right] d\tau \quad (15)$$

ter deleža gradientnega vektorja: and from parts of the gradient vector:

$$\mathbf{Q}(\omega) = \frac{1}{m\pi} \int_0^{2m\pi} \mathbf{Y}^T \left( 2\omega \frac{d^2 \mathbf{Y}}{d\tau^2} \cdot \mathbf{a} + \frac{\partial \mathbf{h}}{\partial \omega} \right) d\tau \quad (16)$$

in matrike: as well as the matrix:

$$\mathbf{P}(\lambda) = \frac{1}{m\pi} \int_0^{2m\pi} \mathbf{Y}^T \mathbf{G}_{N3} d\tau \quad (17)$$

Enačbo (9) rešujemo iterativno z Newton-Raphsonovim postopkom. Če računamo kakšen posebni primer periodičnega nihanja, sta amplitudna vektorja  $\mathbf{f}_n^c$ ,  $\mathbf{f}_n^s$  znana, prav tako pa sta znana vzbujevalna frekvenca  $\omega$  in vektor prostih parametrov  $\lambda$ . V tem primeru so  $\Delta \mathbf{f}_n^c = \mathbf{0}$ ,  $\Delta \mathbf{f}_n^s = \mathbf{0}$ ,  $\Delta \omega = 0$  in  $\Delta \lambda = \mathbf{0}$ . Če je pri tem še  $\mathbf{R} = \mathbf{0}$ , je rešitev kar začetni približek vektorja  $\mathbf{a}$ . Običajno pa v začetku  $\mathbf{R}$  še ni enak ničelnemu vektorju, zato rešitev enačbe (9) da vektor prirastkov  $\Delta \mathbf{a}$ , s katerim popravimo začetno rešitev  $\mathbf{a}$ . Postopek ponavljamo tako dolgo, dokler norma vektorja  $\mathbf{R}$  ne postane dovolj majhna, oziroma dokler ne izpolnimo predpisanega tolerančnega kriterija. Ko je rešitev izračunana, lahko enačbo (9) uporabimo za izvedbo vrste parametričnih študij. Parametrično študijo izvedemo navadno v odvisnosti od enega samega parametra. Zato enačbo (15) zapišemo v obliki:

$$\Delta \mathbf{F} = \frac{1}{m\pi} \int_0^{2m\pi} \Delta f \left[ \sum_{n=1}^{M_i} \mathbf{Y}^T \left( \mathbf{u}_n^c \cos n\tau - \mathbf{u}_n^s \sin n\tau \right) \right] d\tau \quad (18)$$

in povečevanje vzbujevalne sile izrazimo z enim skalarnim parametrom  $\Delta f$ , kar imenujemo postopek amplitudne povečave. Uporabimo pa lahko tudi povečevanje vzbujevalne frekvence z uporabo enačbe (16), kar ustreza frekvenčni povečavi ali povečevanje enega od prostih parametrov  $\lambda_1, \dots, \lambda_p$  z enačbo:

$$\mathbf{P}(\lambda) \Delta \lambda = \Delta \lambda_i \frac{1}{m\pi} \int_0^{2m\pi} \mathbf{Y}^T \mathbf{G}_{N3} d\tau \cdot \mathbf{v}_i, \quad i \in \{1, \dots, p\} \quad (19)$$

kjer je  $\mathbf{v}_i$  primerno izbran vektor in so vsi where  $\mathbf{v}_i$  is a suitable vector and all  $\Delta \lambda_j$ ,  $j \neq i \wedge j \in \{1, \dots, p\}$  enaki nič. Izvedbo  $\Delta \lambda_j$ ,  $j \neq i \wedge j \in \{1, \dots, p\}$  are equal to zero. Thus, the

Equation (9) is solved iteratively using the Newton-Raphson procedure. For the computation of a particular example of periodic oscillation it is assumed that the amplitude vectors  $\mathbf{f}_n^c$ ,  $\mathbf{f}_n^s$ , the exciting frequency  $\omega$  and the vector of the free parameters  $\lambda$  are known. In this case  $\Delta \mathbf{f}_n^c = \mathbf{0}$ ,  $\Delta \mathbf{f}_n^s = \mathbf{0}$ ,  $\Delta \omega = 0$  and  $\Delta \lambda = \mathbf{0}$ . When the residual vector is also equal to zero,  $\mathbf{R} = \mathbf{0}$ , then we already have a solution that is equal to the initial guess of vector  $\mathbf{a}$ . However, at the beginning of the computation the vector  $\mathbf{R}$  is usually not equal to the zero vector and the solution of Equation (9) gives us an increment vector  $\Delta \mathbf{a}$  to update the initial solution  $\mathbf{a}$ . The procedure is repeated until the norm of vector  $\mathbf{R}$  becomes sufficiently small, which is until the prescribed tolerance is satisfied. When a solution is computed, Equation (9) can be used to perform various kinds of parametric studies. The parametric study is usually carried out for the pendency on one parameter only. From this reason Equation (15) is written in the form:

so that the incrementation of the exciting force, called the amplitude augmentation, is dependent on one scalar parameter  $\Delta f$ . Of course we can use an incrementation of the exciting frequency through Equation (16) or an incrementation of one of the parameters  $\lambda_1, \dots, \lambda_p$  by using the equation:



parametrične študije tako predstavlja alternativna uporaba iterativnega postopka in povečave.

Po opisanem postopku je mogoče parametrično študijo opraviti na celotnem območju vrednosti parametra le v primeru, ko so vse točke, v katerih se izračun izvaja, regularne. Na žalost temu ni vedno tako. V točkah, kjer je tangentska matrika  $\mathbf{H}$  singularna, vektorja prirastkov  $\Delta \mathbf{a}$  v splošnem ne moremo enolično določiti. Tangentska matrika je singularna v razvejitvenih točkah, vključno z obračališči. Rang tangentske matrike v regularnih točkah je enak  $NN_h$ , v singularnih točkah pa manjši od omenjenega števila. Če tangentsko matriko razširimo s skupnim vektorjem desne strani enačbe (9), je rang tako razširjene matrike v obračališčih spet  $NN_h$ , ne pa tudi v preostalih razvejitvenih točkah. Zato se težavam v obračališčih lahko izognemo z dodatno enačbo, s katero zagotovimo rang  $NN_h+1$  matrike povečanega sistema enačb. Če vzamemo povečanje parametra  $\lambda_i, i \in \{1, \dots, p\}$ , sta preostala dva parametra nespremenljiva,  $\Delta f=0$  in  $\Delta \omega=0$ . (Podobno bi veljalo za druga dva primera). V nadaljevanju označimo izbrani parameter, ki ga v parametrični študiji spreminjamo s simbolom  $\lambda$ . Namesto parametrizacije s parametrom  $\lambda$ , ki v obračališčih odpove, uvedemo parametrizacijo po ločni dolžini iskane krivulje. To parametrizacijo uvedemo z enačbo:

$$g(\mathbf{a}, \lambda) - s = 0 \quad (20),$$

kjer je  $s$  ločni parameter in  $g(\mathbf{a}, \lambda)$  funkcija, ki jo navadno izberemo v obliki  $g(\mathbf{a}, \lambda) = \mathbf{a}^T \mathbf{a} + \lambda^2$ . Rang  $NN_h+1$  v obračališčih zagotovimo z enačbo (20) ob uvedbi majhnih motenj:

$$g(\mathbf{a} + \Delta \mathbf{a}, \lambda + \Delta \lambda) - (s + \Delta s) = g(\mathbf{a}, \lambda) + \frac{\partial g}{\partial \mathbf{a}} \Delta \mathbf{a} + \frac{\partial g}{\partial \lambda} \Delta \lambda - s - \Delta s = 0 \quad (21),$$

pri čemer se razširjeni sistem enačb glasi:

$$\begin{bmatrix} \mathbf{H} & \mathbf{P} \\ \frac{\partial g}{\partial \mathbf{a}} & \frac{\partial g}{\partial \lambda} \end{bmatrix} \begin{Bmatrix} \Delta \mathbf{a} \\ \Delta \lambda \end{Bmatrix} = \begin{Bmatrix} \mathbf{R} \\ s + \Delta s - g(\mathbf{a}, \lambda) \end{Bmatrix} \quad (22),$$

oziroma:

$$\mathbf{J}_x \cdot \Delta \mathbf{x} = \mathbf{r}, \quad \mathbf{J}_x = \begin{bmatrix} \mathbf{H} & \mathbf{P} \\ \frac{\partial g}{\partial \mathbf{a}} & \frac{\partial g}{\partial \lambda} \end{bmatrix}, \quad \Delta \mathbf{x} = \begin{Bmatrix} \Delta \mathbf{a} \\ \Delta \lambda \end{Bmatrix}, \quad \mathbf{r} = \begin{Bmatrix} \mathbf{R} \\ s + \Delta s - g(\mathbf{a}, \lambda) \end{Bmatrix} \quad (23).$$

Matrika  $\mathbf{J}_x$  je Jacobijeva matrika, ki je regularna v obračališčih, vendar še vedno singularna v točkah podvojitve period. Tangenta v teh točkah ni enolična, zato so točke podvojitve period tista mesta v razvejitvenem diagramu, kjer nastajajo nove veje stabilnih subharmoničnih rešitev. Če predpostavimo, da prvotna smer krivulje določa tangento  $dx/ds$  na stabilno periodično rešitev, sestavljeno iz lihih in sodih harmonikov, nadaljevanje v smeri te tangente prinese prav tako, vendar nestabilno rešitev. Problem je tedaj samo v določitvi tangente na stabilno subharmonično rešitev. To tangento določimo iz enačbe:

realization of the parametric study is represented by the alternative use of the iterative procedure and the augmentation.

In this way the parametric study can be made on the entire domain of parameter values, when the computation is realized in regular points. Unfortunately, this is not always the case. At points where the tangential matrix  $\mathbf{H}$  is singular the increment vector  $\Delta \mathbf{a}$  generally cannot be uniformly determined. The tangential matrix is singular at bifurcation points, including folds. The rank of the tangential matrix in regular points is equal to  $NN_h$ , but it is smaller at singular points. When the tangential matrix is expanded by the overall right-hand side vector of equation (9), the rank of such an expanded matrix is again equal to  $NN_h$  in turning points, but not in others. For this reason difficulties in turning points can be avoided by means of an additional equation, so that the rank  $NN_h+1$  of the expanded system of the equation is ensured. When we choose the augmentation of parameter  $\lambda_i, i \in \{1, \dots, p\}$ , the remaining two parameters are constant,  $\Delta f=0$  and  $\Delta \omega=0$ . (Similar conclusions also hold for two other cases). In the sequel we denote the selected parameter, which is varied in the parametric study by the symbol  $\lambda$ . Instead of a parametrization with parameter  $\lambda$ , which fails in the turning points, we introduce the parametrization by the arc length of curve. This parametrization is introduced by the equation:

where  $s$  is an arc length parameter and  $g(\mathbf{a}, \lambda)$  is function, which is usually selected in the form  $g(\mathbf{a}, \lambda) = \mathbf{a}^T \mathbf{a} + \lambda^2$ . The rank  $NN_h+1$  in turning points is ensured by a small perturbation in Equation (20):

where the expanded system of the equation reads:

or:

Matrix  $\mathbf{J}_x$  is a Jacobian matrix, which is regular in turning points, but is still singular in period doubling points. Because the tangent in these points is not unique, period doubling points are places of the bifurcation diagram where new branches of stable subharmonic solutions emanate. When we suppose that the original direction of the curve determines the tangent  $dx/ds$  on the stable periodic solution, which is composed from odd and even harmonics, then a continuation in the tangent direction brings a quite similar, but unstable, solution. The problem then is how the tangent on the stable subharmonic solution can be computed. This tangent is determined from the equation:

$$\frac{d\mathbf{x}_2}{ds} = \frac{d\mathbf{x}_1}{ds} + \gamma \mathbf{b} \quad (24).$$

Pri tem sta  $\mathbf{b}$  in  $\mathbf{c}$  desni oziroma levi lastni vektor enačb  $\mathbf{J}_x \mathbf{b} = \mathbf{0}$  in  $\mathbf{c}^T \mathbf{J}_x = \mathbf{0}^T$ ,  $\gamma$  pa je skalar, ki zadošča enačbi:

Here  $\mathbf{b}$  and  $\mathbf{c}$  mean the right- and left-hand eigenvectors of equations  $\mathbf{J}_x \mathbf{b} = \mathbf{0}$  and  $\mathbf{c}^T \mathbf{J}_x = \mathbf{0}^T$ , respectively, and  $\gamma$  is a scalar that satisfies the equation:

$$\gamma = \mathbf{c}^T \cdot \left( \frac{d\mathbf{x}_2}{ds} - \frac{d\mathbf{x}_1}{ds} \right) \quad (25).$$

Iz pogoja:

From the condition:

$$\mathbf{c}^T \mathbf{J}_{xx} \frac{d\mathbf{x}}{ds} \frac{d\mathbf{x}}{ds} = 0 \quad (26),$$

kjer  $\mathbf{J}_{xx}$  označuje tenzor tretjega reda, izpeljemo enačbo:

where  $\mathbf{J}_{xx}$  denotes a tensor of third order, we derive the equation:

$$\gamma = - \frac{2\mathbf{c}^T \mathbf{J}_{xx} \frac{d\mathbf{x}_1}{ds} \mathbf{b}}{\mathbf{c}^T \mathbf{J}_{xx} \mathbf{b} \mathbf{b}} \quad (27),$$

s katero določimo  $\gamma$  in s tem tudi tangento  $d\mathbf{x}_2/ds$ .

which determines the scalar  $\gamma$  and therefore the tangent  $d\mathbf{x}_2/ds$ , too.

### 1.1 Van der Pol–Duffingovo nihalo

### 1.1 Van der Pol–Duffing oscillator

Če vzamemo dinamični sistem z eno prostostno stopnjo,  $N=1$  in izberemo nelinearno funkcijo:

When we take a dynamic system with one degree of freedom,  $N=1$ , and choose the nonlinear function:

$$\mathbf{h} \left( \mathbf{q}(t), \frac{d\mathbf{q}}{dt}, \omega, \lambda \right) = h \left( q(t), \frac{dq}{dt}, \omega, \lambda \right) = -\varepsilon (1 - q^2) \frac{dq}{dt} + \Omega_0^2 q + \alpha q^3 \quad (28),$$

z vektorjem prostih parametrov  $\lambda = \{\varepsilon, \Omega_0, \alpha\}^T$ , preide enačba (1) v enačbo van der Pol–Duffingovega nihala:

where  $\lambda = \{\varepsilon, \Omega_0, \alpha\}^T$  denotes the vector of free parameters, then Equation (1) goes into the equation of the van der Pol–Duffing oscillator:

$$\frac{d^2 q}{dt^2} - \varepsilon (1 - q^2) \frac{dq}{dt} + \Omega_0^2 q + \alpha q^3 = \sum_{n=1}^{M_i} (f_n^c \cos n\omega t - f_n^s \sin n\omega t) \quad (29).$$

Pri tem sta vektorja  $\mathbf{f}_n^c$  in  $\mathbf{f}_n^s$  prešla v skalarja  $f_n^c$  oziroma  $f_n^s$ , pa tudi matriki  $\mathbf{G}_{N1}$  in  $\mathbf{G}_{N2}$  sta se reducirali v skalarja:

Here the vectors  $\mathbf{f}_n^c$  and  $\mathbf{f}_n^s$  become scalars  $f_n^c$  and  $f_n^s$ , respectively, and the matrices  $\mathbf{G}_{N1}$  and  $\mathbf{G}_{N2}$  are reduced to scalars as well:

$$\mathbf{G}_{N1} = G_{N1} = \frac{\partial h}{\partial \dot{q}} = \frac{\partial h}{\partial \left( \frac{dq}{d\tau} \right)} = -\varepsilon [1 - q^2(\tau)] \quad (30),$$

$$\mathbf{G}_{N2} = G_{N2} = \frac{\partial h}{\partial q} = 2\varepsilon \omega q(\tau) \frac{dq}{d\tau} + \Omega_0^2 + 3\alpha q^2(\tau)$$

medtem ko matrika  $\mathbf{G}_{N3}$  preide v vrstični vektor:

while matrix  $\mathbf{G}_{N3}$  expands into a row vector:

$$\mathbf{G}_{N3} = \frac{\partial h}{\partial \lambda} = \left\{ [q^2(\tau) - 1] \omega \frac{dq}{d\tau}, 2\Omega_0 q(\tau), q^3(\tau) \right\} \quad (31).$$

Z majhnimi spremembami lahko obravnavamo van der Polovo ali Duffingovo nihalo samo. V enačbo van der Polovega nihala:

With small changes we can treat the van der Pol or Duffing oscillators individually. Equation (29) goes into the equation of the van der Pol oscillator:

$$\frac{d^2 q}{dt^2} - \varepsilon (1 - q^2) \frac{dq}{dt} + \Omega_0^2 q = \sum_{n=1}^{M_i} (f_n^c \cos n\omega t - f_n^s \sin n\omega t) \quad (32)$$

preide enačba (29) tedaj, ko postavimo parameter  $\alpha=0$ . Enačbo Duffingovega nihala:

when parameter  $\alpha$  is set to equal  $\alpha=0$ . We get the equation of the Duffing oscillator:

$$\frac{d^2 q}{dt^2} + \varepsilon \frac{dq}{dt} + \Omega_0^2 q + \alpha q^3 = \sum_{n=1}^{M_i} (f_n^c \cos n\omega t - f_n^s \sin n\omega t) \quad (33)$$

pa dobimo, če namesto funkcije  $\mathbf{h}$  po enačbi (28) izberemo funkcijo:

when we choose, instead of function  $\mathbf{h}$  in Equation (28), the following function:

$$\mathbf{h}\left(\mathbf{q}(t), \frac{d\mathbf{q}}{dt}, \omega, \lambda\right) = h\left(q(t), \frac{dq}{dt}, \omega, \lambda\right) = \varepsilon \frac{dq}{dt} + \Omega_0^2 q + \alpha q^3 \quad (34).$$

Ker je funkcija  $\mathbf{h}$  po enačbi (34) enostavnejša, se poenostavimo izrazi za matriki  $\mathbf{G}_{N1}$  in  $\mathbf{G}_{N2}$  ter vrstični vektor  $\mathbf{G}_{N3}$ :

Because function  $\mathbf{h}$  according to Equation (34) is simplified, then the expressions for the matrices  $\mathbf{G}_{N1}$  and  $\mathbf{G}_{N2}$ , as well as for the row vector  $\mathbf{G}_{N3}$ , simplify, too:

$$\begin{aligned} \mathbf{G}_{N1} = G_{N1} &= \frac{\partial h}{\partial \left(\frac{dq}{d\tau}\right)} = \varepsilon \\ \mathbf{G}_{N2} = G_{N2} &= \frac{\partial h}{\partial q} = \Omega_0^2 + 3\alpha q^2(\tau) \\ \mathbf{G}_{N3} = G_{N3} &= \frac{\partial h}{\partial \lambda} = \left\{ \omega \frac{dq}{d\tau}, 2\Omega_0 q(\tau), q^3(\tau) \right\} \end{aligned} \quad (35).$$

Z izbiro najvišjega reda harmonikov, ki jih upoštevamo v analizi, sta določeni matriki  $\mathbf{T}$  in  $\mathbf{Y}$ , s tem pa je mogoče izračunati tudi matriko  $\mathbf{H}$  po enačbi (10), vektorje  $\mathbf{R}, \Delta\mathbf{F}$  in  $\mathbf{Q}$  po enačbah (14), (16) in (18) ter matriko  $\mathbf{P}$  po enačbi (17). Po izračunu teh matrik in vektorjev se lahko lotimo reševanja enačbe (9), kakor je opisano.

By selecting the highest order of harmonics that are considered in the analysis, the matrices  $\mathbf{T}$  and  $\mathbf{Y}$  are determined. Therefore, the matrix  $\mathbf{H}$  can be computed by Equation (10), the vectors  $\mathbf{R}, \Delta\mathbf{F}$  and  $\mathbf{Q}$  can be computed according to Equations (14), (16), and (18), and the matrix  $\mathbf{P}$  can be computed using Equation (17). After this we can solve Equation (9) as described earlier.

## 2 STABILNOST REŠITEV IN RAZMEJITEV PODROČIJ STABILNOSTI

## 2 THE STABILITY OF THE SOLUTIONS AND A DETERMINATION OF THE BOUNDARIES OF STABILITY REGIONS

Ko je periodična rešitev izračunana, želimo ugotoviti stabilnost rešitve iz dveh pomembnih razlogov. Prvi je ta, da moremo stabilne veje ločiti od nestabilnih, drugi pa, da lahko s spremljanjem lastnih vrednosti prehodne matrike in njihovim prehajanjem prek kroga enote ugotovimo naravo razvejitvenih točk.

When a periodic solution is computed, we want to establish the stability of the solution for two important reasons. The first reason is that stable branches can be distinguished from the unstable ones, and the second reason is that the monitoring of the eigenvalues of the transition matrix with respect to their passing across the unit circle can serve to help find the nature of the bifurcation points.

Stabilnost periodične rešitve ugotovimo z uporabo Floquetove teorije [3]. V ta namen zapišemo enačbo (2) za majhne spremembe v okolici rešitve in dobimo:

The stability of the periodic solution is ascertained by the application of the Floquet theory [3]. For this purpose Equation (2) is written for small perturbations in the vicinity of the solution:

$$\omega^2 \frac{d^2 \Delta \mathbf{q}}{d\tau^2} + \omega \mathbf{G}_{N1} \frac{d\Delta \mathbf{q}}{d\tau} + \mathbf{G}_{N2} \Delta \mathbf{q} = \mathbf{0} \quad (36).$$

Če uvedemo vektor  $\mathbf{z} = \{\Delta \mathbf{q}, \Delta \dot{\mathbf{q}}\}^T$ , lahko zgornjo enačbo zapišemo z uporabo prehodne matrike stanj kot sistem enačb prvega reda:

When we introduce a vector  $\mathbf{z} = \{\Delta \mathbf{q}, \Delta \dot{\mathbf{q}}\}^T$ , then Equation (36) can be rewritten by means of a state transition matrix as a system of first-order equations:

$$\dot{\mathbf{z}} = \mathbf{X}(\tau) \mathbf{z}, \quad \mathbf{X}(\tau) = \begin{bmatrix} \mathbf{0} & \mathbf{I} \\ -\frac{1}{\omega^2} \mathbf{G}_{N2} & -\frac{1}{\omega} \mathbf{G}_{N1} \end{bmatrix} \quad (37).$$

Prehodna (ali monodromna) matrika  $\mathbf{Z}(\tau)$ , ki pripada periodični rešitvi, je matrična rešitev enačbe:

The transition (or monodromy) matrix  $\mathbf{Z}(\tau)$ , which corresponds to the periodic solution, is a matrix solution of the equation:

$$\dot{\mathbf{Z}} = \mathbf{X}(\tau) \mathbf{Z}, \quad \mathbf{Z}(0) = \mathbf{I} \quad (38),$$

katere lastne vrednosti  $\mu_1, \dots, \mu_N$  so Floquetovi množitelji. Kadar so moduli vseh lastnih vrednosti prehodne matrike manjši od 1, je rešitev stabilna, sicer je nestabilna. Ker so lastne vrednosti prehodne matrike v splošnem lahko kompleksne, jih primerjamo

and  $\mu_1, \dots, \mu_N$  are its eigenvalues, which are called Floquet multipliers. When the moduli of all the eigenvalues of the transition matrix are less than 1, the solution is stable, otherwise it is unstable. Because the eigenvalues of the transition matrix can be complex in general, they are



z enotskim krogom. Obračališče ali točka izgube simetrije v razvejitvenem diagramu se pojavi, ko ena od realnih lastnih vrednosti prestopi krog enote skozi točko +1. Točko podvojitve periode imamo, če ena od realnih lastnih vrednosti prestopi krog enote skozi točko -1. Hopfovo razvejitveno točko pa imamo, če krog enote prestopita dve konjugirano kompleksni lastni vrednosti.

Monodromno matriko izračunamo ob koncu periode periodičnega nihanja. Najpreprostejši postopek za izračun prehodne matrike je predlagal Friedmann [3], pri katerem periodo razdelimo na  $N_k$  intervalov, kjer je  $\Delta_k = \tau_k - \tau_{k-1}$ ,  $k=1, \dots, N_k$  trajanje  $k$ -tega intervala. Na vsakem teh intervalov matriko prehajanja stanj  $\mathbf{X}(\tau)$  zamenjamo z nespremenljivo matriko  $\mathbf{X}_k$ :

$$\mathbf{X}_k = \frac{1}{\Delta_k} \int_{\tau_{k-1}}^{\tau_k} \mathbf{X}(\zeta) d\zeta \quad (39)$$

in prehodno matriko  $\mathbf{Z}$  na koncu periode določimo po obrazcu:

$$\mathbf{Z}(2\pi m) = \prod_{i=1}^{N_k} e^{A\mathbf{X}_i} = \prod_{i=1}^{N_k} \left( \mathbf{I} + \sum_{j=1}^{N_j} \frac{(\Delta_i \mathbf{X}_i)^j}{j!} \right) \quad (40)$$

compared in passing through a unit circle. The turning point or symmetry breaking point in the bifurcation diagram occurs, when one of real eigenvalues passes the unit circle through the point +1. We have the period doubling point when one of the real eigenvalues passes the unit circle through the point -1. Finally, we have the Hopf bifurcation point when the unit circle is passed by two complex conjugate eigenvalues.

The monodromy matrix is computed at the end of the period of periodic oscillation. The simplest procedure for computing the transition matrix is proposed by Friedmann [3], where the period is divided into  $N_k$  intervals so that  $\Delta_k = \tau_k - \tau_{k-1}$ ,  $k=1, \dots, N_k$  denotes the duration of the  $k$ -th interval. On each of these intervals the state transition matrix  $\mathbf{X}(\tau)$  is replaced by the constant matrix  $\mathbf{X}_k$ :

and the transition matrix  $\mathbf{Z}$  at the end of the period is determined by the formula:

### 3 ZGLEDI

### 3 EXAMPLES

#### 3.1 Resonančne krivulje

Vzemimo obojestransko členkasto vpet nosilec, kakršen je prikazan na sliki 1. Na obeh koncih je nosilec obremenjen z nespremenljivo tlačno osno silo  $P$  in na upogib s harmonično silo  $F(x, t)$ . Upogibna obremenitev je poleg od časa odvisna še od krajevne koordinate  $x$ , kjer  $x$  zavzame vrednosti  $0 \leq x \leq L$ . Majhne odmike nosilca  $w(x, t)$  od ravnovesne lege opišemo z enačbo [4]:

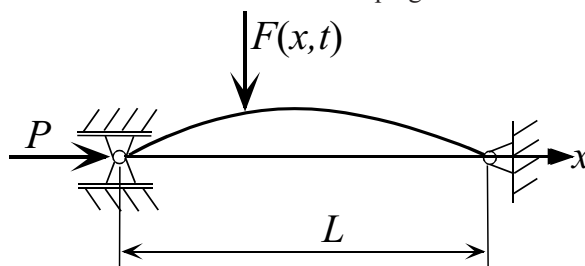
$$\rho A \frac{\partial^2 w}{\partial t^2} + C \frac{\partial w}{\partial t} + \left( P - \frac{EA}{2L} \int_0^L \left( \frac{\partial w}{\partial x} \right)^2 dx \right) \frac{\partial^2 w}{\partial x^2} + EI \frac{\partial^4 w}{\partial x^4} = F(x, t) \quad (41)$$

kjer so:  $L$  dolžina nosilca,  $A$  prečni prerez nosilca,  $E$  modul elastičnosti,  $I$  vztrajnostni moment prereza nosilca,  $\rho$  masa na enoto dolžine nosilca in  $C$  koeficient dušenja nosilca.

#### 3.1 Resonance curves

Consider the hinged-hinged beam shown in the Fig.1. The beam is loaded at both ends with a constant, compressive axial force  $P$ , and at the same time it is loaded by the bending force  $F(x, t)$  with a harmonic time dependence. Besides the time dependence, the bending force is also dependent on the spatial coordinate  $x$ , which takes values in the interval  $0 \leq x \leq L$ . Small deflections  $w(x, t)$  of the beam from equilibrium are described by means of Equation [4]:

where  $L$  is the beam length,  $A$  is the cross-sectional area of the beam,  $E$  is the Young's modulus,  $I$  is the moment of inertia of the beam's cross-sectional area,  $\rho$  is the mass per unit length of the beam and  $C$  is the damping coefficient of the beam.



Sl.1. Upogib nosilca pod vplivom harmonične sile ob hkratni obremenitvi z nespremenljivo tlačno osno silo  
Fig. 1. Bending of the beam under the influence of the harmonic force at simultaneous constant compressive loading along the axis

Na obeh koncih mora nosilec zadostiti robnim pogojem:

Both ends of the beam must fulfil the boundary conditions:

$$w(0,t) = w(L,t) = 0, \quad \frac{\partial^2 w}{\partial x^2}(0,t) = \frac{\partial^2 w}{\partial x^2}(L,t) = 0 \quad (42).$$

Z uvedbo brezrazsežnih spremenljivk:

By introducing nondimensional variables:

$$\bar{x} = \frac{x}{L}, \quad \bar{t} = \frac{1}{L^2} \sqrt{\frac{EI}{\rho A}} t, \quad \bar{\omega} = L^2 \sqrt{\frac{\rho A}{EI}} \omega \quad (43)$$

lahko enačbo (41) prevedemo na obliko:

Equation (41) can be rewritten in the form:

$$\frac{\partial^2 w}{\partial \bar{t}^2} + c \frac{\partial w}{\partial \bar{t}} + \left[ \Gamma - K \int_0^1 \left( \frac{\partial w}{\partial \bar{x}} \right)^2 d\bar{x} \right] \frac{\partial^2 w}{\partial \bar{x}^2} + \frac{\partial^4 w}{\partial \bar{x}^4} = \bar{F}(\bar{x}, \bar{t}) \quad (44),$$

kjer je:

where:

$$c = \frac{CL^2}{\sqrt{\rho A EI}}, \quad \Gamma = \frac{PL^2}{EI}, \quad K = \frac{A}{2I}, \quad \bar{F}(\bar{x}, \bar{t}) = \frac{F(x,t)L^4}{EI} \quad (45).$$

Enačba (44) velja na območju  $0 \leq \bar{x} \leq 1$ . Predpostavimo popolno simetrijo okrog točke  $\bar{x} = \frac{1}{2}$  in vzemimo brezrazsežno upogibno silo v obliki  $\bar{F}(\bar{x}, \bar{t}) = f_n^c \cos n\bar{\omega}\bar{t} \sin \pi\bar{x}$ , ( $n=1,2,\dots$ ). V tem primeru lahko pričakujemo prvo obliko nihanja, to je sinusoidne odmike  $w$  vzdolž koordinate  $\bar{x}$ :

Equation (44) holds in the interval  $0 \leq \bar{x} \leq 1$ . Suppose the full symmetry around the point  $\bar{x} = \frac{1}{2}$  and choose a nondimensional bending force in the form  $\bar{F}(\bar{x}, \bar{t}) = f_n^c \cos n\bar{\omega}\bar{t} \sin \pi\bar{x}$ , ( $n=1,2,\dots$ ). In this case we can expect the first oscillation mode, which is sinusoidal deflections  $w$  along the coordinate  $\bar{x}$ :

$$w(\bar{x}, \bar{t}) = u(\bar{t}) \sin \pi\bar{x} \quad (45).$$

Uvrstitev nastavka (45) v enačbo (44) privede na Duffingovo enačbo, ki opisuje časovno odvisnost pomikov nosilca:

By putting the Ansatz (45) into Equation (44) one obtains the Duffing equation, which describes the time dependence of the beam deflections:

$$\frac{d^2 u}{d\bar{t}^2} + c \frac{du}{d\bar{t}} - \pi^2 (\Gamma - \pi^2) u + \frac{1}{2} K \pi^4 u^3 = f_n^c \cos(n\bar{\omega}\bar{t}) \quad (46).$$

Če brezdimenzijska osna sila zavzame Eulerjevo kritično vrednost  $\Gamma = \pi^2$ , dobi enačba nihanja obliko:

When the nondimensional axial force takes the Euler critical value  $\Gamma = \pi^2$ , the equation takes on the form:

$$\frac{d^2 u}{d\bar{t}^2} + c \frac{du}{d\bar{t}} + \frac{1}{2} K \pi^4 u^3 = f_n^c \cos(n\bar{\omega}\bar{t}) \quad (47).$$

Dobljeni enačbi (46) in (47) lahko rešujemo z opisano metodo koračnega harmonskega ravnovesja. Z zamenjavami  $\varepsilon = c$ ,  $\Omega_0^2 = \pi^2 (\pi^2 - \Gamma)$ ,  $\alpha = K\pi^4/2$  preide enačba (46) v enačbo (33) s poenostavljeno desno stranjo.

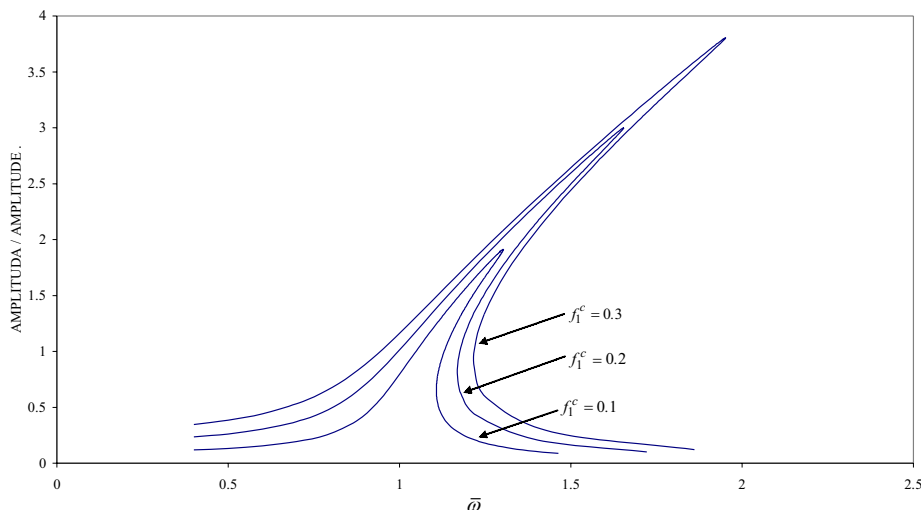
Both Equations (46) and (47) can be solved by the described incremental harmonic balance method. Equation (46) goes by substituting  $\varepsilon = c$ ,  $\Omega_0^2 = \pi^2 (\pi^2 - \Gamma)$ ,  $\alpha = K\pi^4/2$  into Equation (33) with a simplified right-hand side.

V resonančnih krivuljah prikazujemo potek amplitude izbrane harmonske v odvisnosti od spremenljive vzbujevalne frekvence  $\bar{\omega}$ . Na sliki 2 so prikazani poteki resonančnih krivulj družine Duffingovih nihajev za različne vrednosti vzbujevalne amplitude  $f_1^c$ . Izračunani poteki so dobljeni za vrednosti vzbujevalnih amplitud  $f_1^c = 0,1; 0,2; 0,3$ , preostali parametri pa imajo vrednosti  $\varepsilon = 0,04$ ,  $\Omega_0 = 1$  in  $\alpha = 0,25$ . Posamezni potek ustreza nosilcu na sliki 1 in prikazuje frekvenčno odvisnost amplitude prve harmonske. Vrh se pri nosilcu na sliki 1 upogne na desno, ker lahko  $\alpha$  zavzame le pozitivne vrednosti.

Resonance curves show the amplitude course of the selected harmonic with its dependence on the variable exciting frequency  $\bar{\omega}$ . In Fig. 2 the courses of the resonance curves of the family of Duffing oscillators are shown for different values of the exciting amplitude  $f_1^c$ . Computed courses are obtained for the values of the exciting amplitudes  $f_1^c = 0.1; 0.2; 0.3$ , while remaining parameters have values  $\varepsilon = 0.04$ ,  $\Omega_0 = 1$  and  $\alpha = 0.25$ . The particular course corresponds to the beam in Fig. 1 and shows the dependence of the amplitude of the first harmonic on the exciting frequency. The resonance peak of the beam in Fig. 1 is bent to the right according to the positive values of the parameter  $\alpha$ .

Če Duffingovo nihalo sestavlja sistem masa – dušilnik – nelinearna vzmet, lahko parameter  $\alpha$

When the Duffing oscillator is composed of a mass – damper – nonlinear – spring system, the parameter  $\alpha$  can



Sl. 2. Primarna resonanca družine Duffingovih nihaj za različne vrednosti vzbujevalne amplitude  $f_1^c$   
 Fig. 2. Fundamental resonance of the family of Duffing oscillators at various values of the exciting amplitude  $f_1^c$

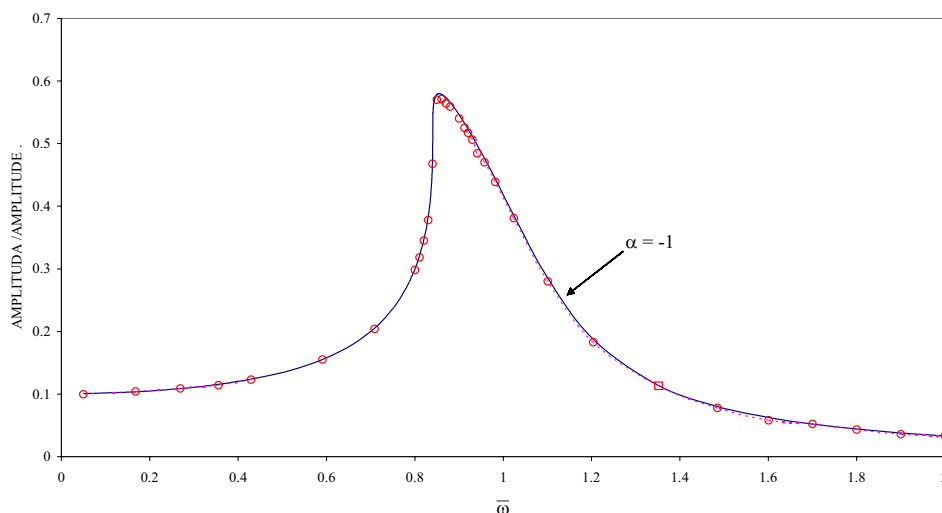
zavzame tako pozitivne kakor negativne vrednosti. Degresivnim karakteristikam vzmeti ustrezajo negativne vrednosti parametra  $\alpha$ , pri čemer se resonančni vrh upogne na levo stran. Progresivnim karakteristikam vzmeti ustrezajo pozitivne vrednosti parametra  $\alpha$  s podobnimi poteki resonančnih krivulj, kakršne so prikazane na sliki 2. Rezultati izračuna resonančne krivulje z MKHR pri degresivnem poteku vzmetne karakteristike so prikazani na sliki 3. Poudariti velja, da potrebujemo za izračun teh krivulj večje število harmonskih kakor pri resonančni krivulji s progresivnim potekom vzmetne karakteristike, predvsem pa je treba preverjati konvergenco rešitve. Zgodi se, da se vrednosti Fourierjevih koeficientov pri višjih harmonskih počasi zmanjšujejo proti nič, zaradi česar je treba v vrsti obdržati dovolj veliko členov. Resonančna krivulja Duffingovega nihala na sliki 3 je izračunana z uporabo MKHR, kjer je v Fourierjevi vrsti poleg nespremenljivega člana upoštevano še 5 harmonskih. Izbrane vrednosti parametrov Duffingovega nihala v analizi so  $\varepsilon=0,2$ ,  $\Omega_0=1$ ,  $\alpha=-1$ ,  $f_1^c=0,1$ . Celoten potek resonančne krivulje je preverjen z numerično integracijo po metodi Runge-Kutta, pri čemer se rezultati obeh metod praktično ujemajo.

Slika 4 prikazuje resonančne krivulje družine van der Polovih nihaj z majhno vrednostjo parametra  $\varepsilon$  in lastno frekvenco nedušenega nihanja linearnega sistema  $\Omega_0=1$ . V izračunu predpostavimo šibko vzbujanje, pri čemer se amplitude zunanega harmoničnega vzbujanja izražajo z  $\varepsilon$  v obliki  $f_1^c = \varepsilon f$ . Na ta način je omogočena primerjava s perturbacijskimi metodami. Z uporabo Lindstedt-Poincaréjeve metode [5] dobimo za primarno resonanco van der Polovega nihala enačbo:

$$\left[ \left( \Omega_0^2 - \omega^2 + \frac{3}{4} \alpha A^2 \right)^2 + \varepsilon^2 \omega^2 \left( 1 - \frac{1}{4} A^2 \right)^2 \right] A^2 = \varepsilon^2 f^2 \quad (46),$$

take positive as well as negative values. The negative values of parameter  $\alpha$  correspond to the soft characteristics of the nonlinear springs where the resonance peak bends to the left-hand side. The hard characteristics of the nonlinear springs correspond to the positive values of the parameter  $\alpha$ , and the resonance curves have similar courses, as shown in Fig. 2. The results of the computation of the resonance curve, which corresponds to the soft-spring characteristic using the IHBM, are shown in Fig. 3. It is worth mentioning that the computation of the resonance curve with a soft characteristic requires a larger number of harmonics than the computation of the resonance curve with hard characteristic, but first of all the convergence of the solution must be examined. It is a fact that values of the Fourier coefficients at higher harmonics decrease slowly towards zero, so that a sufficient number of terms must be retained in the series. The resonance curve of the Duffing oscillator in Fig. 3 is computed by IHBM, where five harmonics are taken into consideration in addition to a constant term. The selected values of the parameters of the analyzed Duffing oscillator are  $\varepsilon=0,2$ ,  $\Omega_0=1$ ,  $\alpha=-1$ ,  $f_1^c=0,1$ . The entire course of the resonance curve is checked by the numerical integration using the Runge-Kutta method, with which it is ascertained that the results of both methods are in good agreement.

Fig. 4 shows the resonance curves of a family of van der Pol oscillators with a small value of parameter  $\varepsilon$  and the natural frequency of the undamped oscillation of a linear system  $\Omega_0=1$ . In the computation a weak excitation is assumed, where the amplitudes of the external harmonic excitation are presented in the form  $f_1^c = \varepsilon f$ . In this way a comparison with the perturbation method is made possible. By applying the Lindstedt-Poincaré method [5] one obtains the following equation for the fundamental resonance of the van der Pol oscillator:



Sl. 3. Primarna resonanca Duffingovega nihala z degresivnim potekom vzmetne karakteristike pri vrednostih parametrov  $\varepsilon=0,2$ ,  $\Omega_0=1$ ,  $\alpha=-1$ ,  $f_1^c = 0,1$  (— rezultati, dobljeni z MKHR, —o—o— rezultati, dobljeni z numerično integracijo po metodi Runge-Kutta)

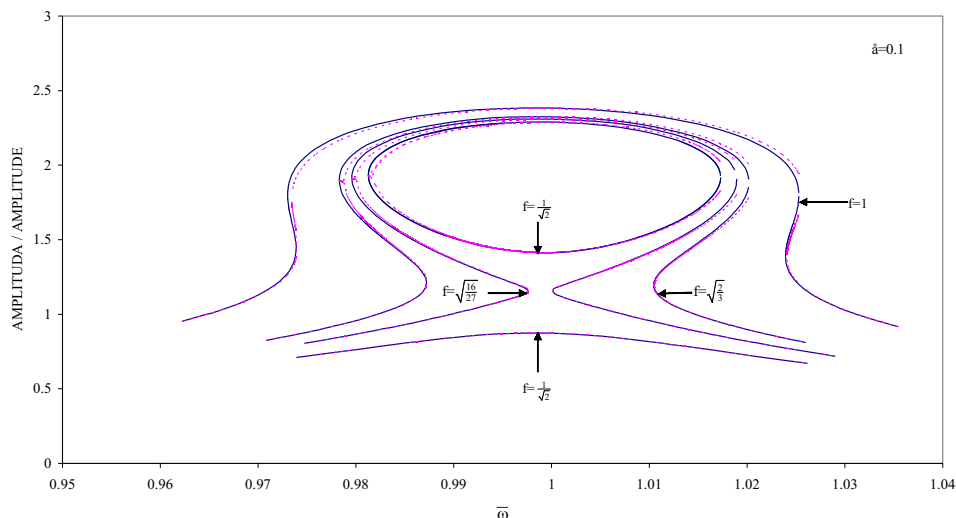
Fig. 3. Fundamental resonance of Duffing oscillator with a soft spring characteristic for values of parameters  $\varepsilon=0,2$ ,  $\Omega_0=1$  and  $\alpha=-1$ ,  $f_1^c = 0,1$  (— results obtained by IHBM, —o—o— results obtained by numerical integration using the Runge-Kutta method)

kjer je  $A = \sqrt{a_1^2 + b_1^2}$  amplituda prve harmonske. Primerjava pokaže popolno ujemanje, če izračun z MKHR izvedemo z omejitvijo na eno samo harmonsko (ker se obe metodi tedaj ujemata) in manjša odstopanja pri večjem številu uporabljenih harmonskih. Rezultati z MKHR na sliki 4 so dobljeni s štirimi harmonskimi in dodatnim nespremenljivim členom v Fourierjevi vrsti pri vrednostih parametrov  $\varepsilon=0,1$ ,  $\Omega_0=1$ ,  $\alpha=0$  ter  $f = 1; \sqrt{2/3}; \sqrt{16/27}; 1/\sqrt{2}$ . Dobljene rezultate MKHR moramo zaradi uporabe večjega števila harmonskih šteti za natančnejše od rezultatov perturbacijskih metod, poleg dejstva, da smemo MKHR brez omejitev uporabiti tudi pri velikih vrednostih parametra  $\varepsilon$ .

Resonančne krivulje so pri velikih vzbujevalnih amplitudah enolične, pri majhnih amplitudah pa večlične. Večličnost je posledica razvejitev. Pri vzbujanju  $f=1$  se pojavita dve histerezi, ki sta posledici parov obračalnih točk. Histerezi se pojavljata v frekvenčnih področjih  $\omega < \Omega_0=1$  in  $\omega > \Omega_0=1$  in sta še bolj izraziti, če je vzbujanje manjše, na primer  $f = \sqrt{2/3}$ . V okviru dosegljive natančnosti ugotovimo, da se pri vzbujanju  $f = \sqrt{16/27}$  obe histerezi praktično skleneta pri frekvenci  $\omega = \Omega_0=1$ . Pri vzbujanjih, ki so manjša od navedene vrednosti, se resonančna krivulja loči na dve veji, pri čemer je zgornja veja oblikovana v sklenjeno zanko. Primer izolirane zanke vidimo pri vrednosti vzbujevalne amplitude  $f = 1/\sqrt{2}$ , ki se v frekvenčnem območju  $0,9815 < \omega < 1,0173$  pojavlja skupaj z ločeno spodnjo vejo resonančne krivulje.

where  $A = \sqrt{a_1^2 + b_1^2}$  is the amplitude of the first harmonic. The comparison shows perfect accordance with the IHBM computation, with the limitation of a single harmonic only (because both methods coincide), and small deviations for a larger number of used harmonics. The results with IHBM in Fig. 4 are obtained with four harmonics and an additional constant term in the Fourier series at values of parameters  $\varepsilon=0,1$ ,  $\Omega_0=1$ ,  $\alpha=0$  and  $f = 1; \sqrt{2/3}; \sqrt{16/27}; 1/\sqrt{2}$ . The obtained results of the IHBM are expected to be more accurate than the results of the perturbation methods because of the larger number of applied harmonics, as well as the fact that the IHBM can be applied without limitation for higher values of parameter  $\varepsilon$ .

The resonance curves are uniform at very high values of excitation amplitudes and multi-variate at small amplitudes. The multi-valuedness is the result of bifurcations. Two hysteresis appear at the excitation  $f=1$ , which are the consequence of pairs of turning points. Hystereses appear in the frequency domains  $\omega < \Omega_0=1$  and  $\omega > \Omega_0=1$  and become more pronounced at smaller excitations, for instance at  $f = \sqrt{2/3}$ . In the frame of attainable accuracy it is ascertained that both hystereses are practically touched at the frequency  $\omega = \Omega_0=1$ , when the excitation takes the value  $f = \sqrt{16/27}$ . At excitation levels that are smaller than the mentioned critical value, the resonance curve is split into two branches, where the upper branch forms the closed loop. The example of the isolated loop is shown at the value of excitation amplitude  $f = 1/\sqrt{2}$ , which appears in the frequency range  $0.9815 < \omega < 1.0173$  together with the separated lower branch of the resonance curve.



Sl. 4. Resonančne krivulje van der Polovega nihala pri različnih vrednostih vzbujevalne amplitude in parametru  $\varepsilon=0,1$  (— rezultati, dobljeni z MKHR, ---- rezultati, dobljeni s perturbacijskimi metodami)  
 Fig. 4. Resonance curves of the van der Pol oscillator at various values of the exciting amplitude and parameter  $\varepsilon=0.1$  (— results obtained by IHBM, ---- results obtained by perturbation methods)

### 3.2 Parametrična študija nosilca, obremenjenega na upogib z upoštevanjem Eulerjeve kritične vrednosti brezrazsežne tlačne sile vzdolž osi nosilca

Pri nosilcu na sliki 1 nas ne zanimajo le resonančne krivulje, temveč tudi upogib nosilca v odvisnosti od amplitude vzbujevalne sile. Razvejitveni diagram kaže v tem primeru delovanje različnih mehanizmov, ki na koncu privedejo celo do kaotičnih nihanj. Primer izračuna takega diagrama z MKHR prikazuje slika 5, v katerem smo predpostavili, da je nosilec obremenjen z brezrazsežno tlačno osno silo, enako Eulerjevi kritični vrednosti  $I=\pi^2$ , na upogib pa s harmonično silo  $\bar{F}(\bar{x}, \bar{t}) = f_2^c \cos 2\bar{\omega}\bar{t} \sin \pi\bar{x} = f \cos 2\bar{\omega}\bar{t} \sin \pi\bar{x}$  ( $n=2$ ). Odziv nosilca pomeni upogibna amplituda ob koncu periode nihanja v odvisnosti od spremenljive amplitude vzbujevalne sile  $f$ . Stabilne rešitve so od nestabilnih ločene z uporabo Floquetove teorije, kakršna je bila opisana v prispevku in prikazana v diagramu s polno oziroma prekinjeno črto. Pri majhnih amplitudah vzbujevalne sile so rešitve simetrične, Fourierjev spekter pa je sestavljen samo iz lihih harmonskih komponent. Rešitve so v začetku stabilne z naraščajočo amplitudo v negativni smeri. Vpliv nelinearnosti se pokaže pri amplitudi vzbujevalne sile  $f=0,46$ , ko postane rešitev nestabilna. Poteku nestabilnih rešitev lahko sledimo le z uporabo metode ločne dolžine, ker nestabilne rešitve oblikujejo zanko ob padajočih vrednostih vzbujevalne amplitude. Rešitev postane ponovno stabilna, ko se vzbujevalna amplituda zmanjša na vrednost  $f=0,23$ . Poteku nove veje stabilnih rešitev sledimo ob povečevanju vzbujevalne amplitude, čemur se upogib nosilca najprej odzove z zmanjševanjem, nato pa s povečevanjem amplitude odziva v pozitivni smeri. Simetrične rešitve, ki vsebujejo le lihe harmonske,

### 3.2 Parametric study of a beam loaded by a bending force with consideration of the Euler critical value of nondimensional compressive force along the beam axis

For the beam in the Fig. 1 the resonance curves are not all that is of interest, the beam bending dependence on amplitude of the exciting force is particularly instructive. The bifurcation diagram in this case shows the working of different mechanisms, which can finally lead even to chaotic oscillations. An example of such diagram, computed by the IHBM, is shown in Fig. 5, where it is supposed that the beam is loaded by a nondimensional compressive force along the axis, which is equal to the Euler critical value  $I=\pi^2$  and is simultaneously subjected to a bending load by the nondimensional bending force  $\bar{F}(\bar{x}, \bar{t}) = f_2^c \cos 2\bar{\omega}\bar{t} \sin \pi\bar{x} = f \cos 2\bar{\omega}\bar{t} \sin \pi\bar{x}$  ( $n=2$ ). The beam response is represented by the bending amplitude at the end of the oscillation period with a dependence on the variable amplitude of the exciting force  $f$ . Stable solutions are separated from unstable ones by means of the Floquet theory, as described in the paper and are diagrammatically shown using continuous and broken lines, respectively. At small amplitudes of the exciting force the solutions are symmetrical and the Fourier spectrum is composed from odd harmonic components only. From the beginning the solutions are stable, with increasing amplitudes in the negative direction. The influence of nonlinearity is indicated at the amplitude of the exciting force  $f=0.46$ , where the solution becomes unstable. The course of the unstable solutions can only be followed by the arc length method because of the loop that is formed at decreasing values of the exciting force. The solution regains its stability when the exciting amplitude decreases to the value of  $f=0.23$ . A new branch of stable solutions follows when the exciting amplitude is



postanejo nestabilne, ko vzbujevalna amplituda doseže vrednost  $f=2,39$ . Ena od lastnih vrednosti v tej točki je  $+1$ , kar pomeni, da se je pojavila prekinitev simetrije. Nestabilnim rešitvam ustreza ena od realnih lastnih vrednosti, ki presega vrednost  $+1$  in jim v diagramu sledimo s prekinjeno črto ob nadaljnjem povečevanju vzbujevalne amplitude. Zaradi prekinitve simetrije nastane dve novi veji stabilnih rešitev, ki poleg lihih vsebujeta še sode harmonske. Omenjeni stabilni rešitvi sta asimetrični. Pri vzbujevalni amplitudi  $f=3,29$  nastane nov par asimetričnih rešitev. Ko vzbujevalna amplituda doseže vrednost  $f=5,38$ , postaneta asimetrični rešitvi nestabilni, pri čemer ena od realnih lastnih vrednosti prekorači vrednost  $-1$ . Nestabilni asimetrični rešitvi dobimo z nadaljnjim povečevanjem vzbujevalne amplitude. Hkrati pa imamo v tej točki podvojitve periode, to je nastanek stabilnih subharmoničnih rešitev z dvojno periodo oziroma Fourierjevim spektrom, ki vsebuje poleg sodih in lihih komponent tudi subharmonične komponente v obliki celoštevilčnih mnogokratnikov polovične osnovne frekvence. Če vzbujevalno amplitudo še naprej povečujemo, nastanejo nadaljnje razvejitve, ki privedejo do stabilnih subharmoničnih rešitev višjega reda. Ko več ne dobimo nobenih stabilnih subharmoničnih rešitev višjega reda, obstajajo v ustreznem območju le še kaotične rešitve. V obravnavanem primeru se področje kaotičnih nihanj začne pri vrednosti vzbujevalne amplitude  $f=6,5$ .

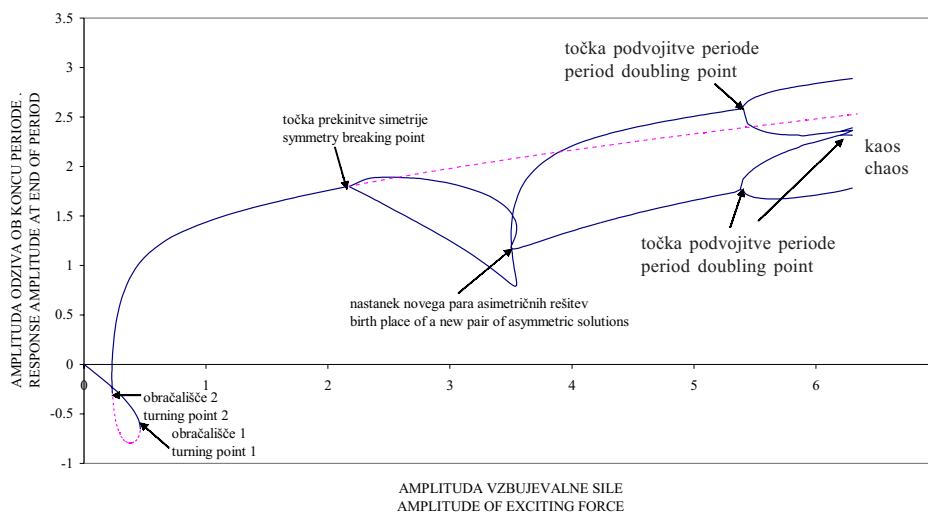
increased, where the beam bending responds initially by reducing the response amplitude and after that by increasing the response amplitude in a positive direction. Symmetrical solutions that contain only odd harmonics become unstable at a value of exciting amplitude  $f=2.39$ . One of the real eigenvalues at this point reaches the value  $+1$ , which means that symmetry breaking occurs. Unstable solutions have one of the eigenvalues greater than  $+1$  and are diagrammatically followed by the broken line when the exciting amplitude is further increased. Due to the symmetry breaking two new branches of the stable solutions occur, which contain odd and even harmonics. These two stable solutions are asymmetric. At the value of the exciting amplitude  $f=3.29$  a new pair of asymmetric solutions is formed. When the exciting amplitude reaches the value  $f=5.38$  the asymmetric solutions become unstable, where one of the real eigenvalues crosses the value  $-1$ . Unstable asymmetric solutions are obtained by further increasing the exciting amplitude. At the same time we have period doubling in the bifurcation point, which means that stable subharmonic solutions with a double period are formed, which have Fourier spectra containing even, odd and subharmonic components. When the exciting amplitude is further increased, subsequent bifurcations arise, which lead to subharmonic solutions of a higher order. When no stable subharmonic solutions of a higher order exist, then only chaotic solutions are possible in the corresponding region. In the above example, the chaotic region starts at a value of exciting amplitude  $f=6.5$ .

#### 4 SKLEP

V prispevku je prikazana prilagoditev MKHR, ki omogoča sledenje po vejah razvejitvenega diagrama v primerih, ko postane tangenta (Jacobijeva) matrika sistema algebrajskih enačb

#### 4 CONCLUSION

This paper presents an adaptation of the IHBM, which makes it possible to follow the path along branches of the bifurcation diagram when a tangential (Jacobian) matrix of algebraic system equations becomes



Sl. 5. Razvejitveni diagram upogibnega odziva nosilca v odvisnosti od vzbujevalne amplitude (— stabilna rešitev, ---- nestabilna rešitev)

Fig. 5. Bifurcation diagram of beam bending response with the dependence on exciting amplitude (— stable solution, ---- unstable solution)

singularna. Med singularnimi točkami razvejitvenih diagramov so obravnavane obračalne točke, točke prekinitve simetrije in točke, v katerih prihaja do podvojitve period. Adaptacija MKHR je uporabljena pri van der Pol-Duffingovem nihalu. Obojestransko členkasto vpet nosilec, obremenjen z nespremenljivo tlačno osno silo  $P$  in na upogib s harmonično silo  $F(x,t)$  je obravnavan kot Duffingovo nihalo. Prikazan je izračun primarne resonance družine Duffingovih in van der Polovih nihal v odvisnosti od vzbujevalne frekvence in različnih vrednosti vzbujevalnih amplitud. Pri Duffingovem nihalu je prikazan tudi izračun primarne resonance z regresivno karakteristiko nelinearne vzmeti. Parametrična študija obravnavanega nosilca v odvisnosti od amplitude vzbujevalne sile kaže scenarij, ki vodi od simetričnih periodičnih nihanj do razvejitve, v kateri postanejo rešitve asimetrične, nato pa se nadaljuje s sekvenco razvejitev, ki ustrezajo podvojitvam period, dokler sistem ne zaniha kaotično. Simetrična periodična nihanja pripadajo Fourierjevemu spektru, ki vsebuje samo lihe harmonične komponente, asimetrična periodična nihanja vsebujejo poleg lihih še sode komponente, nihanjem s podvojeno periodo pripadajo subharmonične rešitve, območje kaotičnih nihanj pa ustreza področju, v katerem ne obstaja nobeno stabilno subharmonično nihanje višjega reda več.

singular. Among the singular points of bifurcation diagrams, turning points, symmetry breaking points and period doubling points are treated. An adaptation of the IHBM is applied on the van der Pol-Duffing oscillator. A hinged-hinged beam, loaded with both a constant compressive axial force  $P$  and a harmonic bending force  $F(x,t)$  is treated as a Duffing oscillator. The computation of the fundamental resonance of the family of Duffing and van der Pol oscillators with the dependence on exciting frequency is shown for different values of exciting amplitudes. In the case of the Duffing oscillator the computation of fundamental resonance with the soft characteristic of a nonlinear spring is also shown. A parametric study of the analyzed beam with the dependence on the amplitude of the exciting force shows a scenario that leads from symmetric periodic oscillations to the bifurcation, where solutions become asymmetric and continue with a sequence of bifurcations, corresponding to the period doublings until the system oscillates in the chaotic region. The symmetric periodic oscillations correspond to the Fourier spectrum, which contains only odd harmonic components, asymmetric periodic oscillations contain odd and even harmonic components, period doubling oscillations correspond to the subharmonic solutions; and finally, the region of chaotic oscillations corresponds to the domain where no stable subharmonic oscillation of a higher order does not exist.

## 5 LITERATURA 5 REFERENCES

- [1] Pušenjak, R. (1997) Analiza nelinearnih oscilatorjev z več prostostnimi stopnjami – Analysis of nonlinear oscillators with finite degrees of freedom. *Strojniški vestnik*. 43,5-6, 219-230.
- [2] Seydel, R. (1994) Practical bifurcation and stability analysis. From equilibrium to chaos. Second Edition; New York, *Springer-Verlag*.
- [3] Friedmann, P., C.E. Hammond, and T.-H. Woo (1977) Efficient numerical treatment of periodic systems with application to stability problems. *International Journal for Numerical Methods in Engineering*; 11, 1117-1136.
- [4] Kramer, B., R. Pušenjak (1999) Stabilitás és a tartó frekvenciamenetének meghatározása növekményes harmonikus linearizálás módszerével, *Járművek*. Evf. 46, 7/8, 57-60.
- [5] Pušenjak, R. (2001) Kombinacijske resonance v sistemih s kvadratičnimi nelinearnostmi z razširjeno Lindstedt-Poincaréjevo metodo. Zbornik del Kuhljevi dnevi '01, 129-136, Ljubljana: Slovensko društvo za mehaniko.

Avtorjev naslov: Dr. Rudolf Pušenjak  
Univerza v Mariboru  
Fakulteta za strojništvo  
Smetanova 17  
2000 Maribor  
rudi.pusenjak@uni-mb.si

Author Address: Dr. Rudolf Pušenjak  
University of Maribor  
Faculty of Mechanical Eng.  
Smetanova 17  
2000 Maribor, Slovenia  
rudi.pusenjak@uni-mb.si

Prejeto: 9.4.2003  
Received:

Sprejeto: 12.9.2003  
Accepted:

Odprto za diskusijo: 1 leto  
Open for discussion: 1 year